Journal of
Materials Chemistry C

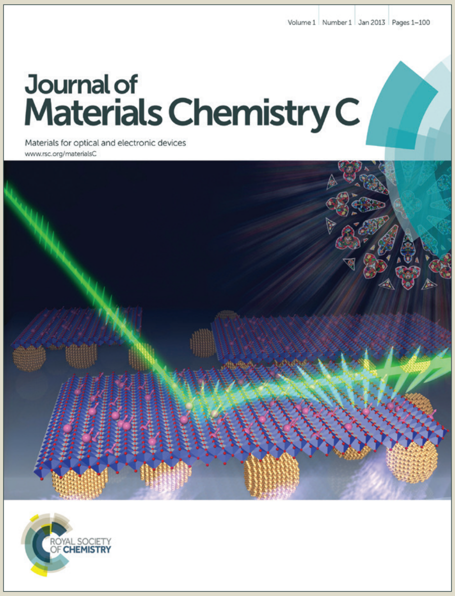

Journal Name

ARTICLE

Silver Embedded Nanostars for SERS with Internal Reference (SENSIR)

Received 00th January 20xx,
Accepted 00th January 20xx

DOI: 10.1039/x0xx00000x

www.rsc.org/

Andrew M. Fales[a,b] and Tuan Vo-Dinh[a,b,c,*]

We report the synthesis of a unique hybrid nanoplatform consisting of silver-embedded gold nanostars that entraps a reference dye between the gold and silver surfaces, providing an internal reference signal for quantitative surface-enhanced Raman scattering (SERS) analysis without the need for aggregation. The unique geometry of the nanostar provides SERS enhancement in a non-aggregated state for analytes on the exterior surface of the particle. When an equivalent structure was created using gold nanospheres as the core, no SERS signal from the analyte was observed until aggregation was induced by the addition of salt. Rhodamine 6G (Rh6G) was used as a model analyte to demonstrate this proof of concept. The use of the internal standard to reduce SERS signal variability was demonstrated in a highly scattering medium and at various particle concentrations, to simulate conditions that may be encountered with real-world samples. This novel, internal reference containing nanostructure will aid quantitative SERS analysis in complex media.

Introduction

Surface-enhanced Raman scattering (SERS) has emerged as a powerful spectroscopic tool for biological, chemical, and environmental analyses. Raman scattering is highly specific, providing a fingerprint-like spectrum of the vibrational modes in a molecule. The inherently weak Raman scattering of molecules can be enhanced by multiple orders of magnitude when placed within a few nanometers of a plasmonic nanostructure to generate SERS. Our laboratory has been investigating a wide variety of SERS-active platforms,[1-4] ranging from metal film on nanoparticle-coated microplates, nanorod arrays, nanodots, nanowires, and nanostars.[5-7] While SERS has been shown to offer single-molecule detection sensitivity, quantification becomes an issue if the SERS platform is not reproducible. This is very evident when using colloidal solutions of nanospheres, as they rely on aggregation to provide SERS enhancement.[8]

Recent developments in the synthesis of anisotropic nanoparticles have led to shapes that no longer require aggregation to generate SERS, such as nanocubes, nanorods, and nanostars.[6, 7, 9, 10] These types of particles contain sharp points that concentrate the electromagnetic field, acting as intrinsic hot spots for SERS.[3] Of these different shapes, gold nanostars have been shown to provide the highest SERS enhancement.[11] Although quantitative SERS analysis has been greatly improved by the use of anisotropic nanoparticles, there are still cases where the use of an internal standard would be necessary to obtain reliable data from a sample.

There have been reports concerning the use of an internal reference for SERS analysis, but none have involved nanostars or other anisotropic nanoparticles. The isotope edited internal standard method is perhaps the most accurate, though it requires an analyte that can be isotope-edited to produce shifted SERS peaks.[12] This manuscript is focused on SERS nanoparticles that contain their own internal reference signal, requiring no additional modification of the analyte or sample preparation. The synthesis of SERS nanoparticles with embedded dye labels has been accomplished in a variety of ways. One method involved filling an Au-Ag nanoshell with the reference dye, then overcoating with silver.[13] Another used dye-labeled polyelectrolytes to coat gold nanoparticles, which were then embedded into a silver shell.[14] DNA has been used to create gold nanoparticles with a 1-nm, dye-containing interior gap.[15] The strategy to embed thiolated molecules between the core and shell of a metal nanoparticle is what we have employed in this manuscript.[16, 17]

Herein, we report the design of internal reference containing, silver-embedded gold nanostars and demonstrate their ability to reduce SERS signal variation due to matrix effects. The synthesis is a modified version of our previous report on silver-coated gold nanostars.[18] Unlike spherical nanoparticles, these nanostar-based platforms do not require aggregation to induce SERS, resulting in better reproducibility for quantitative analysis. Internal reference particles were made using

---

[a] Fitzpatrick Institute for Photonics, Duke University, Durham, North Carolina 27708, USA
[b] Department of Biomedical Engineering, Duke University, Durham, North Carolina 27708, USA
[c] Department of Chemistry, Duke University, Durham, North Carolina 27708, USA
* Phone: (919) 660-8520, Fax: (919) 613-9145, Email: tuan.vodinh@duke.edu

† Electronic Supplementary Information (ESI) available: Figures S1 and S2 as described in the text. See DOI: 10.1039/x0xx00000x

spherical gold nanoparticles as a control, to establish that the nanostar core is necessary to achieve SERS without aggregation. This is, to the best of our knowledge, the first report of a plasmonic internal reference nanoparticle for non-aggregated SERS.

Experimental

Materials

All chemicals were purchased from Sigma-Aldrich (St. Louis, MO) at the highest purity grade available and used as received unless otherwise specified. Ammonium hydroxide (NH_4OH, 29%), and ethanol (200 proof) were acquired through VWR (Radnor, PA). Polystyrene beads (1.0 µm diameter) were obtained from Polysciences, Inc. (Warrington, PA). Glassware and stir bars were cleaned with *aqua regia* prior to use. Ultrapure water (18MΩ·cm) was used in all preparations.

Instrumentation

UV/Vis extinction spectra were acquired with a FLUOstar Omega plate reader (BMG LABTECH GmbH, Germany). Transmission electron microscopy (TEM) was performed with a FEI Tecnai G^2 twin transmission electron microscope (Hillsboro, OR). Raman spectra were recorded on a Renishaw inVia Raman microscope (Gloucestershire, U.K.) equipped with a 633 nm laser for excitation. Particle concentrations were measured with a Nanosight NS500 (Malvern Instruments Ltd, Worcestershire, U.K.).

Spherical gold nanoparticle synthesis (AuNP)

The AuNP were prepared using the citrate reduction method. An Erlenmeyer flask (250 mL) containing 100 mL of 0.25 mM $HAuCl_4$ was brought to a boil while stirring vigorously. To this solution, 0.8 mL of 1% w/v trisodium citrate dihydrate in water was quickly injected. The solution immediately became colorless, gradually changed to dark grey, and then finally to a dark purple. After this point the solution was kept boiling for 30 minutes, then cooled to room temperature before use. The as-prepared particles were then labeled with *para*-mercaptobenzoic acid (pMBA, 10 µM final concentration), along with the addition of Tween 20 (0.02% final concentration) and left overnight. The particles were washed by centrifugation at 2000 rcf for 60 minutes and redispersed into 0.02% Tween 20 solution.

Gold nanostar synthesis (AuNS)

The AuNS were synthesized as previously reported. Briefly, a 10 mL solution of 0.25 mM HAuCl4 containing 10 µL of 1 N HCl was prepared in a 20 mL scintillation vial. With rapid stirring, 100 µL of 12 nm gold seed was quickly added to the above solution. After even dispersion of the gold seed (~5 s), 50 µL of 0.1 M ascorbic acid and 50 µL of 20 mM AgNO3 were rapidly and simultaneously added, and the color of the solution changed from a pale red to deep blue. A final concentration of 10 µM pMBA and 0.02% Tween 20 were then added and allowed to incubate overnight. The sample was then washed by centrifugation at 2000 rcf for 20 minutes and resuspended in 0.02% Tween 20.

Silver embedding of gold nanostars (AuNS@Ag) and spherical nanoparticles (AuNP@Ag)

For 1 mL of the pMBA labeled nanostars, equivalent amounts (1, 3, 5, 7, or 10 µL) of 0.1M $AgNO_3$ (designated Ag1, Ag3, Ag5, Ag7, Ag10, respectively) and 0.1M ascorbic acid were added sequentially and vortexed to mix. The silver reduction process was initiated by the addition of 2 µL NH_4OH (29%), causing the extinction spectrum of the solution to begin blue shifting. The reaction was allowed to proceed for at least one hour prior to using the particles in subsequent experiments. The AuNS@Ag5 were selected for further study as they provided the maximum internal standard signal observed; AuNP@Ag5 were prepared for control experiments.

Model analyte SERS detection

Rhodamine 6G (Rh6G) was used as a model analyte to demonstrate the SERS activity on the exterior surface of AuNS@Ag and AuNP@Ag. The prepared particles (~0.1nM concentration) were mixed with Rh6G dissolved in ethanol to achieve final concentrations in the range of 1 to 10 µM. The samples were transferred to glass vials for measurement on the Renishaw microscope. The laser (~6.8 mW at the sample) was focused into the solution with a 10x objective, and a 10 second exposure time was used to record the Raman spectrum. In the case of the AuNP@Ag, no SERS from Rh6G was observed when the particles were non-aggregated; to achieve a measureable Rh6G signal, 5 mM $MgCl_2$ was added to the solution immediately before collecting the spectrum to induce aggregation.

Demonstration of reduced SERS variability by using an internal standard

The variability of SERS signal in a scattering medium was investigated by adding 1.0 µm polystyrene beads to solutions of 0.1 nM AuNS@Ag containing 10 µM Rh6G. After mixing, the solutions were transferred to glass vials for the Raman measurements as previously described.

We also studied the effect of particle concentration on the measured SERS signal. A range of AuNS@Ag concentrations from 20 to 100 pM were prepared and 10 µM final concentration of Rh6G was added. The samples were transferred to glass vials and Raman spectra were acquired as above.

Results and Discussion

The procedure to prepare the nanostars with internal reference is similar to our previous report of silver-coated gold nanostars.[18] In this case, the gold nanostars were labeled with 4-mercaptobenzoic acid (pMBA) prior to the silver coating process. The thiol functionality of pMBA allows it to bind strongly with the gold surface through the formation of Au-S bonds. Tween 20, a non-ionic surfactant, was used to stabilize the particles during the washing and silver coating steps. The pMBA-labeled nanostars then served as seed particles for the silver growth, with silver nitrate used as the silver precursor and ascorbic acid as the reducing agent. While in the presence of 0.02% Tween 20, this reduction process proceeds very slowly at room temperate and neutral pH. Ammonium hydroxide was used to increase the pH of the solution and speed up the reaction rate. The particles were left undisturbed for at least one hour prior to further experiments.

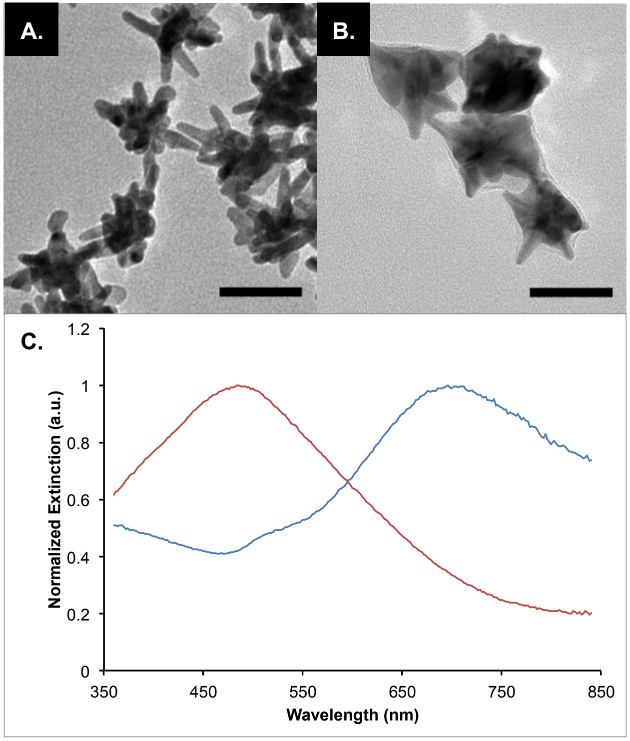

Figure 1. TEM images of gold nanostars (A) and silver-coated gold nanostars (B). The extinction spectra of the gold nanostars (blue) and silver-coated gold nanostars (red) are shown in (C). Scale bars are 50 nm.

The silver coating was monitored via UV/Vis absorption spectroscopy and TEM. Figure 1A,B shows the TEM images of gold nanostars before and after being coated with silver. It can be seen that the silver growth occurs mainly on the core of the gold nanostar, allowing the 'hot-spot' branches to remain accessible to external analytes. The extinction spectra of gold nanostars and silver-coated gold nanostars are shown in Figure 1C, with the gold nanostar plasmon starting in the NIR at ~700 nm, and blue-shifting down to ~485 nm after the silver coating. These findings are consistent with our previous work and indicate that embedding of the pMBA between the gold nanostar core and silver shell does not have a significant effect on the obtained particle morphology.

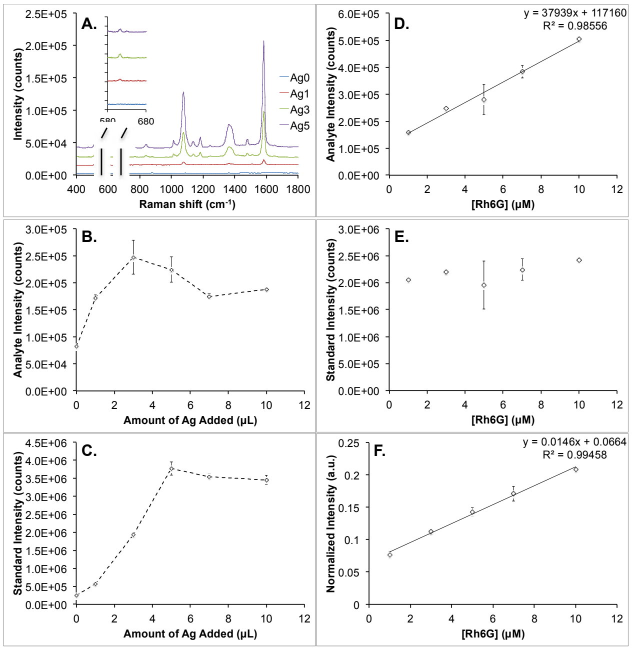

Figure 2. (A) SERS spectra of pMBA functionalized gold nanostars with different amounts of silver; inset zoomed in on the 613 cm^{-1} Rh6G peak, (B) Integrated SERS intensity from 10 µM Rh6G, (C) Integrated SERS intensity from embedded pMBA on gold nanostars with different amounts of silver coating. (D) Integrated Rh6G signal intensity, (E) integrated pMBA signal intensity, (F) pMBA normalized Rh6G signal intensity at different concentrations of Rh6G. The spectra in (A) have been offset for clarity. Error bars are ±1 standard deviation.

The SERS intensity of both the embedded pMBA and external Rh6G, selected as a model analyte, were investigated at different amounts of silver coating. Figure 2A contains representative spectra that demonstrate the greatly enhanced pMBA SERS signal that is obtained after embedding the nanostars in different amounts of silver. The integrated intensity of the Rh6G peak at 613 cm^{-1} on nanostars with different amounts of silver coating is shown in Figure 2B. The 1583 cm^{-1} peak of pMBA was also integrated and plotted against the amount of silver added, seen in Figure 2C. After a certain amount of silver coating is reached, both the Rh6G and pMBA signals begin to decrease. For the external Rh6G, once the nanostars become completely embedded in the silver, the nanostar branches can no longer act as hot spots of electromagnetic field enhancement, resulting in a decrease of the SERS signal. The embedded pMBA signal increases rapidly up to the point where most of the gold surface has been covered in silver; after this point, there is a gradual decrease in signal as the silver coating is increased, suggesting that the signal is resulting from pMBA molecules embedded between the gold surface and silver coating. This is further evidenced by functionalizing AuNS@Ag with pMBA on the outer surface instead of the gold surface before coating, resulting in about two orders of magnitude lower signal (Figure S1). Thus, pMBA can be used as an internal reference to normalize the signal from analytes on the surface of the particle, reducing variability due to environmental factors. The Ag5 sample (as defined in the experimental section) with the highest pMBA signal was selected for further measurements and is what was shown in Figure 1.

The SERS enhancement factor (EF) for the internal standard and external analyte on the SENSIR particles was determined using pMBA. A 0.1 M solution of pMBA in 1 M NaOH was used as the Raman standard. For the external EF, 1 µM pMBA was added to AuNS@Ag that were prepared without embedded pMBA. These spectra can be found in Figure S1, along with a description of the EF calculation. The internal EF was determined using AuNS-pMBA@Ag synthesized with 1 µM pMBA embedded. The calculated external EF was 4.1×10^4, matching our previous report on gold nanostars.[19] We found the internal EF to be much higher, as could be observed in Figure 2A, at 4.2×10^6.

While the internal EF provides a very high internal reference signal, this could interfere with the detection of external analytes with low Raman cross-sections. However, we have observed that the presence of the reference signal does not significantly impact the external analyte signal in regions where their peaks do not overlap (Figure S2). When comparing the signal from 10 µM Rh6G on SENSIR particles and AuNS@Ag without embedded reference, the 613 cm^{-1} Rh6G peak intensities are within 10% of each other. It is also possible to tune the nanoparticle structure (size/branching of gold nanostar and amount of silver coating) depending on the wavelength of the laser excitation and/or resonance of the analyte to optimize the SERS enhancement.[18] If spectral overlap of the peaks is an issue, other reference dyes (*i.e.* small thiol molecules) may be used. In our preliminary results, p-aminothiophenol is another dye suitable for embedding (data not shown).

The use of these particles for quantitative detection was demonstrated by establishing a calibration curve for Rh6G concentrations ranging from 1 to 10 µM while the particle concentration used was 0.1 nM. The integrated intensity of Rh6G, pMBA, and the pMBA normalized Rh6G intensity are shown in Figure 2D, Figure 2E, and Figure 2F, respectively. A linear fit was performed on the Rh6G calibration curve, obtaining an R^2 value of 0.986. The normalized Rh6G curve improved the R^2 value to 0.996, demonstrating that even under ideal conditions the use of an internal standard can aid in quantitative measurements.

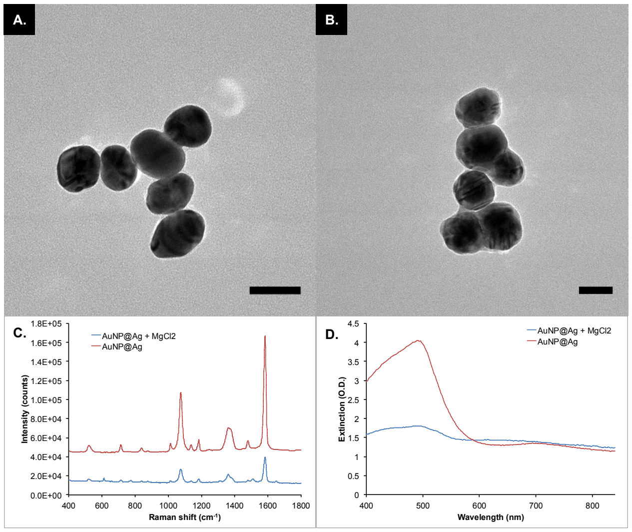

Figure 3. TEM images of gold spheres (A) and silver-coated gold spheres (B). (C) shows the SERS spectra, offset for clarity, of pMBA-embedded silver-coated gold nanospheres with 10 µM Rh6G, before (red) and after (blue) the addition of 5 mM $MgCl_2$. Note the appearance of the 613 cm^{-1} Rh6G peak after $MgCl_2$ addition. (D) is the extinction spectrum of AuNP@Ag with (blue) and without (red) 5 mM $MgCl_2$, indicating rapid aggregation of the particles after salt addition. Scale bars are 50 nm.

To confirm that the nanostar geometry is what provides the unique capability to combine an internal reference signal with the ability to perform non-aggregated SERS analysis on external analytes, a control experiment with gold nanospheres was performed. The 50 nm gold nanospheres were prepared by citrate reduction, resulting in a particle concentration of ~0.1 nM. An image of the particles can be found in Figure 3A. Functionalization with pMBA was performed in the same manner as the nanostars, and silver coating followed the Ag5 protocol from the experimental section. Figure 3B is a TEM image of the silver coated spheres (AuNP@Ag), where the more electron dense gold core is clearly visible through the silver shell. It was observed that no SERS from Rh6G on AuNP@Ag could be obtained unless salt was added to induce nanoparticle aggregation (Figure 3C). The 613 cm-1 peak from Rh6G appears after addition of 5 mM MgCl2 to the solution. In the presence of this salt, the plasmon band of the AuNP@Ag is greatly reduced (Figure 3D), indicative of extensive aggregation in the nanoparticle solution.

The dependence upon aggregation of nanoparticles to produce SERS signals from the AuNP@Ag introduces significant issues with reproducibility. This is very apparent in the calibration curve for Rh6G that was constructed in Figure S3, resulting in a linear fit with an R^2 value of 0.578. The random nature of the aggregation process results in a distribution of monomers, dimers, trimers, and higher clusters, all of which have different SERS enhancements. As such, the internal reference signal can no longer be used to normalize the analyte signal due to the inconsistent SERS enhancement factors throughout the sample. This problem is avoided when using the nanostars in place of spherical nanoparticles; since nanostars have intrinsic hot spots that do not require aggregation, there is a more uniform distribution of SERS enhancement throughout the sample.

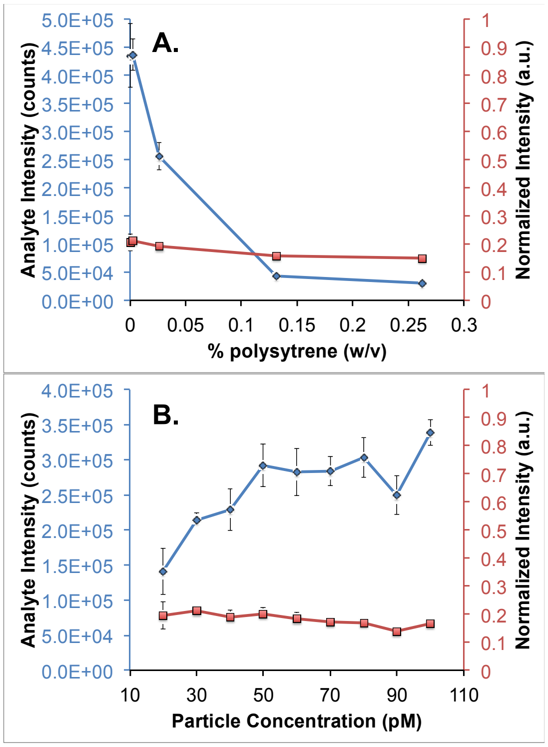

Figure 4. Integrated SERS intensity of 10 μM Rh6G (blue) and the normalized Rh6G intensity (red) when used for analysis in a highly scattering medium (A) and at various particle concentrations (B). Error bars are ±1 standard deviation.

The utility of the internal reference nanostars for reducing SERS signal variability was demonstrated in a highly scattering medium, and also when using different particle concentrations. Polystyrene beads were added at different concentrations to solutions containing 0.1 nM AuNS@Ag and 10 μM Rh6G. This simulates the optically dense environments that are often found in unpurified biological or ecological samples. Figure 4A demonstrates the exponential decay in SERS signal as the concentration of polystyrene beads is increased. The extinction spectra of the polystyrene beads in solution can be found in the supporting data (Figure S4). There is over an order of magnitude change in Rh6G signal intensity going from no polystyrene beads up to 0.26% w/v. Normalizing the signal by the internal reference significantly reduces this variation, with the lowest normalized intensity falling within two standard deviations of the original sample.

In cases where the concentration of SERS nanoparticles may be variable, such as in vivo, where the particles and/or their solvent could diffuse from the site of delivery, the analyte signal will be affected. The effect of particle concentration on signal from 10 μM Rh6G was investigated by varying the AuNS@Ag from 20 pM to 100 pM (Figure 4B). As shown, the Rh6G signal intensity is correlated with the concentration of particles. At the lowest particle concentration tested, Rh6G signal is less than half that at the highest concentration, whereas the normalized Rh6G signal is essentially a flat line; performing a linear fit on the data in Figure 4B gives a slope of -0.0007. In both of these examples, quantification using SERS would be nearly impossible without the use of an internal reference. The obtained results provide a proof of concept for the use of these novel nanoparticle structures for quantitative SERS detection in complex samples.

To further demonstrate this point, we have taken the raw Rh6G intensity and the normalized intensity from Figure 4A at 0.026% polystyrene, and used the calibration curves from Figure 2 to calculate the predicted concentration of Rh6G. These results have been plotted in Figure 5. As shown, the predicted concentration of 10 μM Rh6G is 3.7 ± 0.3 μM when only using the raw signal intensity. After normalization to the pMBA peak, the predicted concentration is now 8.6 ± 0.9 μM, falling within two standard deviations of the actual value. Thus, we have clearly shown how the internal standard signal can aid in quantitative SERS analysis.

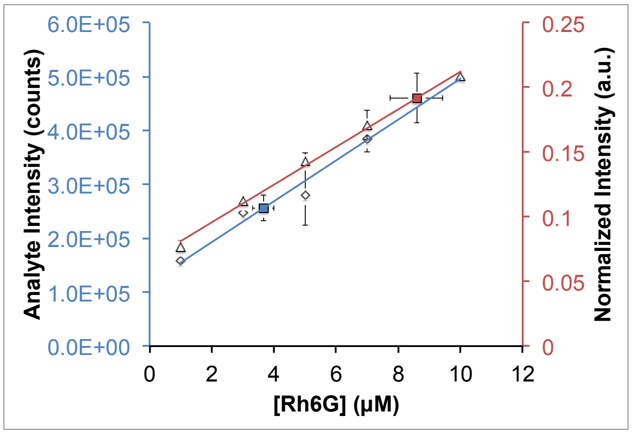

Figure 5. The calibration curves from Figure 2 are plotted together. The Rh6G intensity linear fit is shown in blue, with data points as diamonds (left axis). The normalized linear fit is shown in red, with data points as triangles (right axis). The measured 10 μM Rh6G intensity in 0.026% polystyrene and its predicted concentration is shown as the blue square. The normalized 10 μM Rh6G intensity in 0.026% polystyrene and its predicted concentration is shown as the red square. Error bars are ±1 standard deviation.

Conclusions

We have developed a silver-embedded gold nanostar platform that entraps an internal reference dye between the gold and silver surfaces. The unique geometry of the nanostar provides SERS enhancement in a non-aggregated state for analytes on the exterior surface of the particle. When gold nanospheres were used to create silver-embedded particles, salt had to be added to aggregate the particles before any SERS could be detected from the external analyte. The internal reference was shown to significantly reduce SERS signal variation in a highly scattering sample and at different particle concentrations, conditions that simulate some of the matrix effects that may be encountered in real-world samples. This internal reference nanoparticle structure provides improvement over current strategies for quantitative SERS analysis in complex samples.

Acknowledgements

The authors report no conflict of interest. This work was sponsored by the Defense Advanced Research Projects Agency (HR0011-13-2-0003) and Duke University Exploratory Research Funds. The content of this article does not necessarily reflect the position of the policy of the Government, and no official endorsement should be inferred.

References

1 Vo-Dinh, T.; Liu, Y.; Fales, A. M.; Ngo, H.; Wang, H.-N.; Register, J. K.; Yuan, H.; Norton, S. J.; Griffin, G. D. SERS Nanosensors and Nanoreporters: Golden Opportunities in Biomedical Applications. *Wiley Interdisciplinary Reviews: Nanomedicine and Nanobiotechnology* **2015,** *7*, (1), 17-33.

2 Vo-Dinh, T. Surface-enhanced Raman spectroscopy using metallic nanostructures. *Trends in Analytical Chemistry* **1998,** *17*, (8–9), 557-582.

3 Vo-Dinh, T.; Fales, A. M.; Griffin, G. D.; Khoury, C. G.; Liu, Y.; Ngo, H.; Norton, S. J.; Register, J. K.; Wang, H.-N.; Yuan, H. Plasmonic nanoprobes: from chemical sensing to medical diagnostics and therapy. *Nanoscale* **2013,** *5*, (21), 10127-10140.

4 Vo-Dinh, T.; Hiromoto, M. Y. K.; Begun, G. M.; Moody, R. L. Surface-enhanced Raman spectrometry for trace organic analysis. *Anal. Chem.* **1984,** *56*, (9), 1667-1670.

5 Fales, A. M.; Yuan, H.; Vo-Dinh, T. Silica-Coated Gold Nanostars for Combined Surface-Enhanced Raman Scattering (SERS) Detection and Singlet-Oxygen Generation: A Potential Nanoplatform for Theranostics. *Langmuir* **2011,** *27*, (19), 12186-12190.

6 Khoury, C. G.; Vo-Dinh, T. Gold Nanostars For Surface-Enhanced Raman Scattering: Synthesis, Characterization and Optimization. *J. Phys. Chem. C* **2008,** *112*, (48), 18849-18859.

7 Yuan, H.; Khoury, C. G.; Hwang, H.; Wilson, C. M.; Grant, G. A.; Vo-Dinh, T. Gold nanostars: surfactant-free synthesis, 3D modelling, and two-photon photoluminescence imaging. *Nanotechnology* **2012,** *23*, (7), 075102.

8 Zhang, Y.; Walkenfort, B.; Yoon, J. H.; Schlucker, S.; Xie, W. Gold and silver nanoparticle monomers are non-SERS-active: a negative experimental study with silica-encapsulated Raman-reporter-coated metal colloids. *Phys. Chem. Chem. Phys.* **2015,** 10.1039/C4CP05073H.

9 Sun, Y.; Xia, Y. Shape-Controlled Synthesis of Gold and Silver Nanoparticles. *Science* **2002,** *298*, (5601), 2176-2179.

10 Sau, T. K.; Murphy, C. J. Room Temperature, High-Yield Synthesis of Multiple Shapes of Gold Nanoparticles in Aqueous Solution. *Journal of the American Chemical Society* **2004,** *126*, (28), 8648-8649.

11 Nalbant Esenturk, E.; Hight Walker, A. R. Surface-enhanced Raman scattering spectroscopy via gold nanostars. *J. Raman Spectrosc.* **2009,** *40*, (1), 86-91.

12 Zhang, D.; Xie, Y.; Deb, S. K.; Davison, V. J.; Ben-Amotz, D. Isotope Edited Internal Standard Method for Quantitative Surface-Enhanced Raman Spectroscopy. *Anal. Chem.* **2005,** *77*, (11), 3563-3569.

13 Pinkhasova, P.; Puccio, B.; Chou, T.; Sukhishvili, S.; Du, H. Noble metal nanostructure both as a SERS nanotag and an analyte probe. *Chemical Communications* **2012,** *48*, (78), 9750-9752.

14 Zhou, Y.; Lee, C.; Zhang, J.; Zhang, P. Engineering versatile SERS-active nanoparticles by embedding reporters between Au-core/Ag-shell through layer-by-layer deposited polyelectrolytes. *Journal of Materials Chemistry C* **2013,** *1*, (23), 3695-3699.

15 Lim, D.-K.; Jeon, K.-S.; Hwang, J.-H.; Kim, H.; Kwon, S.; Suh, Y. D.; Nam, J.-M. Highly uniform and reproducible surface-enhanced Raman scattering from DNA-tailorable nanoparticles with 1-nm interior gap. *Nat Nano* **2011,** *6*, (7), 452-460.

16 Gandra, N.; Singamaneni, S. Bilayered Raman-Intense Gold Nanostructures with Hidden Tags (BRIGHTs) for High-Resolution Bioimaging. *Advanced Materials* **2013,** *25*, (7), 1022-1027.

17 Zhou, Y.; Ding, R.; Joshi, P.; Zhang, P. Quantitative surface-enhanced Raman measurements with embedded internal reference. *Analytica Chimica Acta* **2015,** *874*, (0), 49-53.

18 Fales, A. M.; Yuan, H.; Vo-Dinh, T. Development of Hybrid Silver-Coated Gold Nanostars for Nonaggregated Surface-Enhanced Raman Scattering. *J. Phys. Chem. C* **2014,** *118*, (7), 3708-3715.

19 Yuan, H.; Fales, A. M.; Khoury, C. G.; Liu, J.; Vo-Dinh, T. Spectral characterization and intracellular detection of Surface-Enhanced Raman Scattering (SERS)-encoded plasmonic gold nanostars. *J. Raman Spectrosc.* **2013,** *44*, (2), 234-239.

Table of Contents Graphic

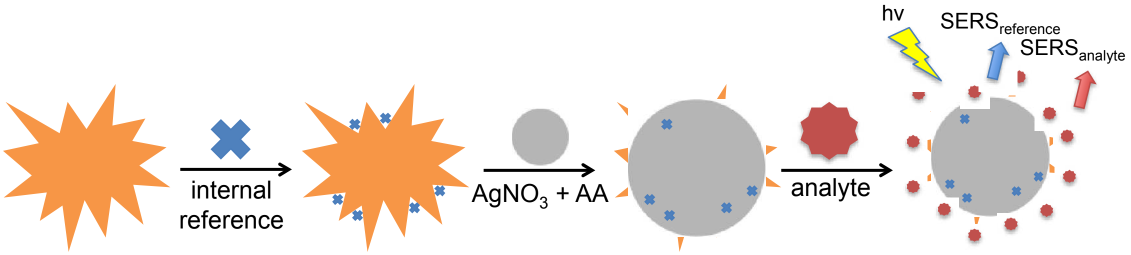

Reference dye labeled nanostars are embedded in a partial silver shell, retaining the sharp gold tips for non-aggregated SERS of external analytes while providing an internal reference signal.